

Fiber optical gyroscope for space applications

Yu.N. Korkishko, V.A. Fedorov, V.E. Prilutskii, V.G. Ponomarev, V.G. Marchuk, I.V. Morev, E.M. Paderin,

S.M. Kostritskii

RPC "OPTOLINK" Ltd., Moscow 124498, Zelenograd, proezd 4806, h.5, Russia
Tel. (+7-495) 536-9933, Fax (+7-495) 536-9934, E-mail: korkishko@optolink.ru

V.N. Branets, V.S. Ryzhkov

S.P. Korolev Rocket and Space Corporation Energia, 141070, Korolev, Moscow region, Russia
Tel. (+7-495) 516-0481, fax (+7-495) 513-6766.

Abstract: The three-axis closed-loop fiber optic gyroscopes are described. The results illustrate the versatility of the technology, showing its potential to meet space grade requirements like compact size and high performance.

OCIS codes: (060.2800); (060.2430)

1. Introduction

Over the last 30 years the interferometric fiber-optic gyroscope (FOG) research and development has evolved from promising experiment to an industrial device used for many applications. FOG is based on the Sagnac effect [1] which states that an optical path length difference is experienced by light beams propagating along opposite directions in a rotating frame. In fiber optical gyroscopes these two counterpropagating waves propagate at closed fiber coil. The obtained phase difference $\Delta\Phi$ is proportional to rotation rate Ω .

Fiber optical gyroscopes are being developed as attractive devices for many navigation and guidance applications. These all solid state devices have many advantages such as light weight, long life time, absence of moving parts and low voltage power.

2. Configuration

The Optolink's TRS-500 FOG consists of the one Superluminescent Light Emission Diode ($\lambda=1550$ nm), three Photodetectors, four Fiber Splitters (1:1) and one Fiber Splitter (1:2) to divide the light into three parts, three ring interferometers to sense three orthogonal angular rates, and printed circuit boards with installed digital signal processor. The ring interferometer consists of a multifunction integrated optic chip (MIOC) and polarization maintaining (PM) fiber coil [2,3]. The MIOC is a three-port optical gyrochip fabricated at lithium niobate wafer by high temperature proton exchange technique [4,5] which provides three functions. First, it polarizes the propagating light to reduce bias instability due to polarization non-reciprocity. Second, it splits the light into clockwise and counterclockwise waves, each with equal optical power and recombines them with a Y-junction waveguide. Third, with electro-optical phase modulator, it applies a biasing phase shift between the counter-propagating beams.

It is well known, that standard technology of PE waveguide (APE-technology) [6] applies a two-level process, which consists of a PE, (melting pure or diluted by lithium benzoate benzoic acid as a rule) and subsequent annealing. It was recently obtained, that different defects are formed in the surface area of waveguide due to different phase transitions [4]. These defects are sources of additional scattering of light.

However, it was recently reported [7], that APE process reduces the electro-optical coefficients and provides a some marked level of propagation loss related mainly to the guide mode leakage. The two primary sources of this leakage are the following: (i) light scattering caused by residual distortion of a near-surface waveguide part, where several phase transitions occur during annealing [8]; and (ii) photorefractive damage [9]. To avoid these undesirable effects, we propose the new method of high temperature proton exchange (HTPE) [4], as there is no any phase transition when the α -phase waveguides are fabricated by HTPE and a concentration of defects, appearing at fabrication process and manifesting themselves as photorefractive centres, are smaller comparatively to the APE process [10]. Finally, this possibility of producing high-quality waveguides with relatively short processing time opens the way for mass production of a large variety of integrated optical components.

TuE91.pdf

Optolink’s PM fiber (PANDA type) is used in order to reduce both the drift caused by the polarization cross coupling and the drift caused by earth’s and outside magnetic field via the Faraday effect.

Quadrupole winding technique implies winding a coil from a single length of fiber, starting at the center of the fiber length, winding outward toward the ends, alternately from one or another of two supply spools, in a geometrically structured way.

Configuration of TRS-500 FOG is presented at Fig.1 and Table 1 summarized its parameters.

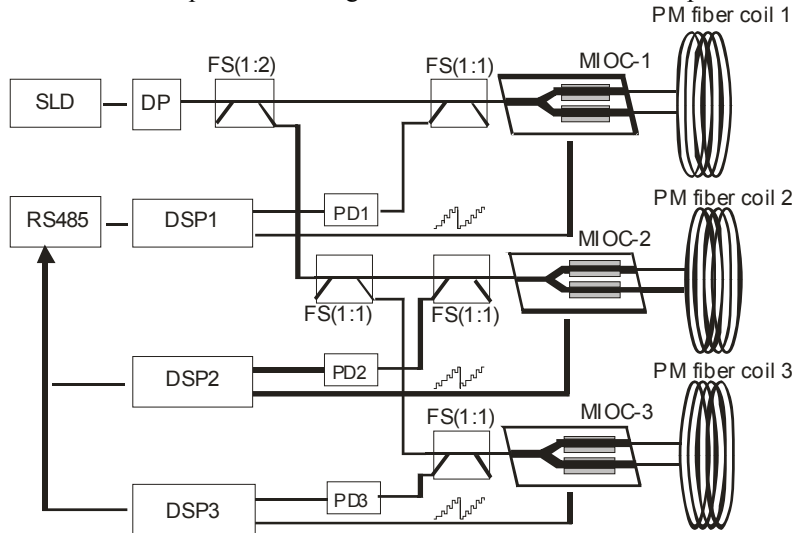


Fig.1. Configuration of TRS-500 gyro.

SLD – superluminescent diode, DP-depolarizer, FS-fiber splitter, DP- depolarizer, FS- fiber splitter, PD– photodetector, MIOC-multifunction integrated optic chip, DSP - digital signal processor.

The TRS-500 FOG uses only one light source – Superluminescent Light Emission Diode with central wavelength $\lambda=1550$ nm, three photodetectors and three digital signal processors (DSP). So, all channels are working simultaneously. Each DSP generates voltage for “sawtooth” light modulation for compensation of Sagnac phase shift and to make fixed phase shift $\pi/2$. As a result, each channel is working in closed-loop regime.

Fig.2 shows the scheme of DSP.

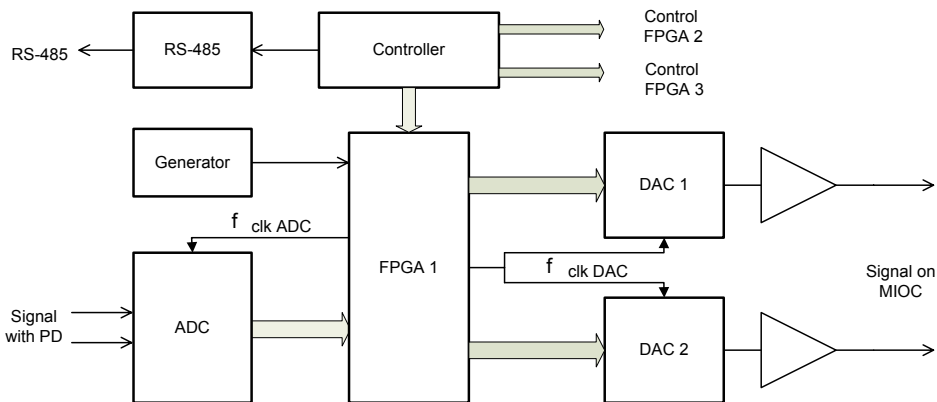


Fig.2. Block diagram of DSP.

ADC - analog to digital converter, DAC- digital to analog converter, FPGA- Field Programmable Gate Array.

Analog signal from analog phase sensitive detector (PSD) that processes the output of the FOG photodetector is amplified and passed to high frequency analog to digital converter (ADC). The digital signal is demodulated by Altera Field Programmable Gate Array (FPGA). Obtained code passed to digital integrator. The code of signal from integrator is using to obtain the slop of phase “saw-tooth” which corresponds to rotation rate. The Digital to Analog

TuE91.pdf

converter creates the analog signal as saw-tooth voltage and pass it to MIOC. The wideband integrated optic phase modulators placed at both arms of MIOC are employed to introduce phase ramp modulation, thus enabling close-loop operation. The loop closure scheme uses a digitally synthesized saw-tooth (serrodyne modulation) of 2π amplitude in optical phase shift. In this case the Sagnac phase shift is compensated by saw-tooth modulation of light with calibrated amplitude 2π and frequency f , determined from well-known equation:

$$f = \frac{D}{n\lambda} \Omega \quad (1)$$

where Ω is a rotation rate, D – diameter of fiber coil, n - effective refractive index of waveguiding mode, λ - wavelength.

The frequency of resulting ramp is then a digital measure of the rotation rate, with each ramp reset proportional to the angular turned, i.e. one ramp is equal to $\frac{n\lambda}{D}$. To increase resolution of gyro the rotation rate is determined by measuring slop of phase saw-tooth.

3. Space testing

The TRS-500 gyro was established into control system of landing module of Russian manned transport spacecraft Soyuz TMA-5, developed and manufactured by S.P.Korolev Rocket and Space Corporation “Energia” in frame of International Space Station program. Flight test has been successfully performed at period from October 2004 to April 2005. The device has been established in the container at the landing module on an arm so, that its sensitivity axes X, Y, Z have been focused parallel to corresponding axes of regular 3-axis electromechanical gyroscope (EMG) with accuracy not worse than $\pm 2^\circ$. Signals «TRS 1», «TRS 2», «TRS 3» were given out from device TRS-500 to the system of the information record proportional to projections of the angular rotation rate to the X, Y and Z axes of the device with a steepness $(0,150 \pm 007)$ V·sec/deg and with ± 20 deg/sec range of the linear zone of measurement. TRS-500 was switched on from the cosmonauts control panel before division of compartments of the landing module and a device-modular compartment.

The performance of fiber optical gyro TRS-500 was estimated from device outputs which are proportional to projections of angular rates to orthogonal axis X, Y, Z of regular device EMG. Fig.3 and Fig.4 show the output of X-axis channel for negative and positive rotation rates. The measured by TRS-500 angular rotation rates were in good agreement with ones measured by regular EMG. Six months flight test showed that FOG TRS-500 was efficiently workable at spacecraft "Souz TMA-5".

After successful flight tests, it was decided to use fiber optical gyros TRS-500 as regular in a landing control system of the spacecrafts “Souz TMA”. At “Soyuz TMA-7” spacecraft, delivered astronauts from International Space Station at April 9th, 2006, the traditional electromechanical gyros were replaced by TRS-500 FOGs.

Table 1. Parameters of TRS-500 FOG.

Range of measured angular rate, °/sec	± 300
Bias drift at fixed temperature, °/h	< 1.0
Scale factor repeatability, %	≤ 0.03
Bandwidth, Hz	300
Random walk, °/√h	$\leq 0,005$
Weight, kg	1.1
Size, mm	110x110x90
Output	RS485

TuE91.pdf

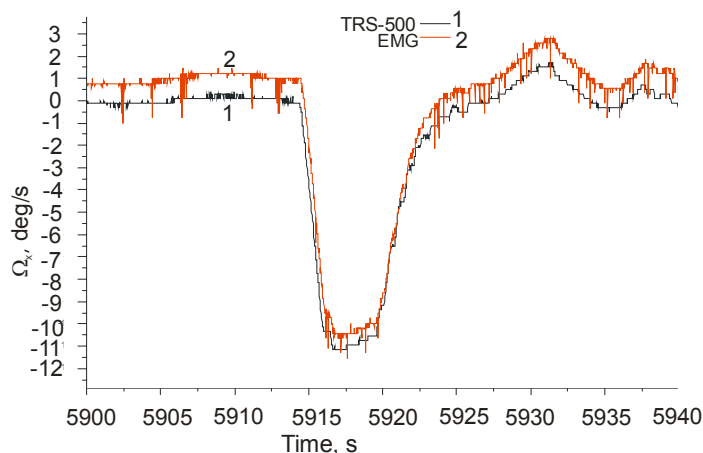


Fig. 3. Output of X-channels of TRS-500 gyro and electromechanical gyro EMG at large negative rotation rates.

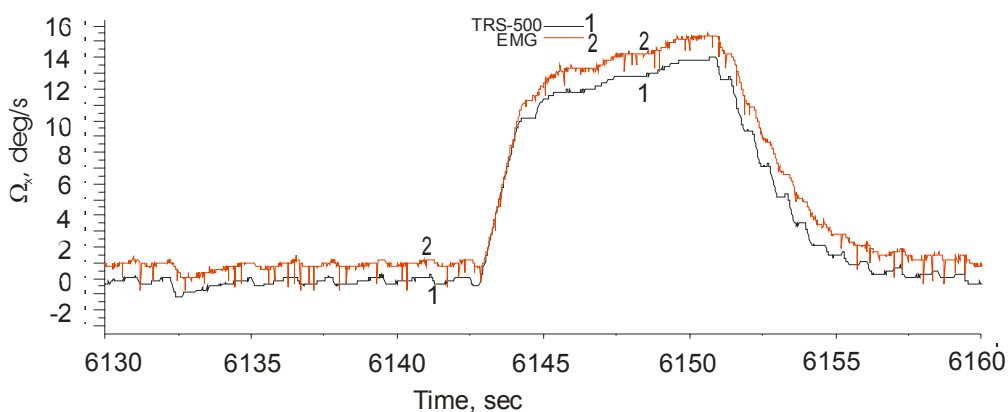


Fig. 4. Output of X-channels of TRS-500 gyro and electromechanical gyro EMG at large positive rotation rates.

4. References

- [1] H.Lefevre, "The Fiber – Optic Gyroscope", Artech House, 1993.
- [2] Yu.N.Korkishko, V.A.Fedorov, V.E.Prilutskii, V.G.Ponomarev, M.A.Fenyuk, V.G.Marchuk, S.M.Kostritskii, E.M.Paderin, "High-precision fiber optical gyro with linear digital output", *Giroskopiya&Navigaziya*, N1, 69-82 (2004).
- [3] V.E.Prilutskii, V.G.Ponomarev, V.G.Marchuk, M.A.Fenyuk, Yu.N.Korkishko, V.A.Fedorov, S.M.Kostritskii, E.M.Paderin, A.I.Zuev, "Interferometric fiber optical gyro with linear output", *Giroskopiya&Navigaziya*, N3, 62-72 (2004).
- [4] Yu.N.Korkishko, V.A.Fedorov, O.Y.Feoktistova, "LiNbO₃ Optical Waveguide Fabrication by High-Temperature Proton Exchange", *J. Lightwave Technology* 18, 562-568 (2000).
- [5] Yu.N.Korkishko, V.A.Fedorov, S.M.Kostritskii, A.N. Alkaev, E.M.Paderin, E.I.Maslennikov, D.V.Apraksin, "Multifunctional integrated optical chip for fiber optical gyroscope fabricated by high temperature proton exchange", *Proc. SPIE* 4944, 262-267 (2003).
- [6] P.G.Suchoski, T.K.Findakly, F.J.Leonberger, "Stable low-loss proton-exchanged LiNbO₃ devices with no electro-optic degradation", *Opt.Lett.* 13, 1050-1052 (1988).
- [7] R. Narayan, "Electrooptic coefficient variation in proton-exchanged and annealed lithium niobate samples", *IEEE. J. of Selected Topics in Quantum Electron.* 3, 796-807 (1997).
- [8] F. Rickermann, D. Kip, B. Gather, and E. Krätzig, "Characterization of photorefractive LiNbO₃ waveguides fabricated by combined proton and copper exchange", *Phys. Stat. Sol. (a)* 150, 763-771 (1995).
- [9] E.E. Robertson, R.W. Eason, Y. Yokoo, and P.J. Chandler, "Photorefractive damage removal in annealed-proton-exchanged LiNbO₃ channel waveguides", *Appl. Phys. Lett.* 70, 2094-2096 (1997).
- [10] A. Erdmann, "The influence of shallow traps on the properties of LiNbO₃ waveguides", *Opt. Commun.* 93, 44-48 (1992).